Synthesis of Stable Ligand-free Gold–Palladium Nanoparticles Using a Simple Excess Anion Method

Meenakshisundaram Sankar,[†] Qian He,[‡] Moataz Morad,[†] James Pritchard,[†] Simon J. Freakley,[†] Jennifer K. Edwards,[†] Stuart H. Taylor,[†] David J. Morgan,[†] Albert F. Carley,[†] David W. Knight,[†] Christopher J. Kiely,[‡] and Graham J. Hutchings[†,*]

[†]School of Chemistry, Cardiff University, Main Building, Park Place, Cardiff, CF10 3AT, U.K., and [‡]Department of Materials Science and Engineering, Lehigh University, 5 East Packer Avenue, Bethlehem, Pennsylvania 18015-3195, United States

ABSTRACT

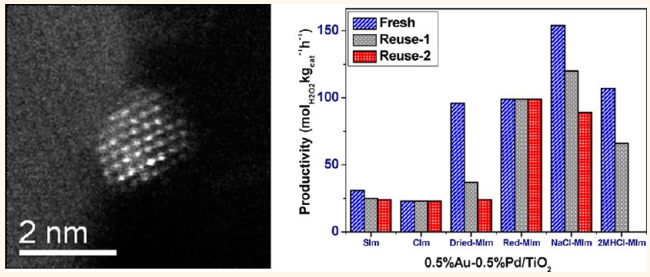

We report a convenient excess anion modification and post-reduction step to the impregnation method which permits the reproducible preparation of supported bimetallic AuPd nanoparticles having a tight particle size distribution comparable to that found for sol-immobilization materials but without the complication of ligands adsorbed on the particle surface. The advantageous features of the modified impregnation materials compared to those made by conventional impregnation include a smaller average particle size, an optimized random alloy composition, and improved compositional uniformity from particle-to-particle resulting in higher activity and stability compared to the catalysts prepared using both conventional impregnation and sol immobilization methods. Detailed STEM combined with EDX analyses of individual particles have revealed that an increase in anion concentration increases the gold content of individual particles in the resultant catalyst, thus providing a method to control/tune the composition of the nanoalloy particles. The improved activity and stability characteristics of these new catalysts are demonstrated using (i) the direct synthesis of hydrogen peroxide and (ii) the solvent-free aerobic oxidation of benzyl alcohol as case studies.

KEYWORDS: modified impregnation · ligand-free synthesis · anion-excess · gold–palladium · direct synthesis of hydrogen peroxide

Supported gold nanoparticles have been found to be effective for a number of applications, including CO oxidation,[1] acetylene hydrochlorination,[2] environmental catalysis,[3−7] energy processing,[8,9] and chemical synthesis.[10−14] For a number of reactions it has been reported recently that bimetallic catalysts exhibit a significant increase in activity as compared to their monometallic analogues.[15−18] For instance, supported gold–palladium catalysts have been found to be very effective for aerobic oxidation reactions[19] and for the direct synthesis of hydrogen peroxide.[13] An important aspect of these catalysts is the size of the supported metal nanoparticles: gold nanoparticles are extremely active catalysts, whereas bulk gold is chemically inert. The method of synthesis of these catalysts is therefore crucial.[20] Many methods for preparing highly active heterogeneous gold and gold–alloy catalysts have been reported to date,[21] including deposition-precipitation,[1,22] chemical vapor deposition,[23] ligand-assisted synthesis,[24] sol-immobilization or colloidal deposition,[25,26] impregnation,[27] and incipient wetness.[28] However, all these methods display one or more of the following disadvantages: (i) a lack of reproducibility of the catalytic activity, (ii) a complex synthesis procedure, (iii) a lack of stability under reaction conditions, or (iv) are applicable/active only for a very specific reaction/support combination. Consequently, considerable effort is still being expended to discover a simple and effective method for the reproducible preparation of highly active and stable gold-based nanoparticulate catalysts.[29,30]

Conventional impregnation (C_{Im}) is the simplest method of making Au–Pd catalysts, but suffers from the great disadvantage of generating materials which display only a moderate level of activity in, for example, the direct synthesis of hydrogen peroxide or the solvent-free oxidation of alcohols.[19,31] For oxide-supported AuPd alloy nanoparticles, detailed analysis of the material by analytical electron microscopy indicated the bimetallic nanoparticles comprised a Au-rich core and Pd-rich shell, with

* Address correspondence to hutch@cardiff.ac.uk.

Received for review December 20, 2011 and accepted July 7, 2012.

Published online July 07, 2012
10.1021/nn302299e

particle sizes typically ranging from 1 to 10 nm, together with occasional very large particles (≫10 nm), and that the smaller particles are the most catalytically active.[19,32] In an attempt to eliminate the catalytically inactive larger particles, many, more sophisticated, preparation methods have been reported in the literature. One such method is sol-immobilization (S_{Im})[25,26] whereby colloidal nanoalloys with a narrow size distribution are prepared using stabilizer ligands and a reducing agent, the colloidal particles being subsequently immobilized onto a metal oxide support. Although this technique results in catalysts having metal particles in the 2−6 nm range and which have a high catalytic activity, this synthetic method is not as simple and versatile as the impregnation technique.[33] Another practical limitation of the sol-immobilization methodology is that it can only be used to prepare Au−Pd catalysts on a very limited number of supports, such as activated carbon and TiO_2, because the efficiency of deposition or immobilization of these preformed colloids is highly dependent on the iso-electric point (IEP) of the support.[33] Furthermore, S_{Im} requires the use of stabilizing ligands and reducing agents, both of which can remain on the surface of the nanoparticles and are potentially deleterious for catalysis.[25,26,34] In addition to these various disadvantages, the sol-immobilization method cannot easily be scaled-up for use on an industrial scale. Very recently, a supramolecular route has been reported for the synthesis of core−shell nanoparticle catalysts, but once again this methodology uses a complicated synthesis procedure for the stabilizer ligand.[24] We have now addressed these problems and define a catalyst synthesis method which is as versatile and simple as the impregnation method, but which results in catalysts as active as those made by sol-immobilization. Here we report that, by adding an excess of the anionic ligands of the metal precursors during an impregnation-type catalyst synthesis, and employing a subsequent heat treatment in a reducing atmosphere, that nanoalloy particles with a very tight particle size and composition distribution are obtained, which are found to be exceptionally active and stable as catalysts for both the direct synthesis of hydrogen peroxide and solvent-free aerobic oxidation of benzyl alcohol.

RESULTS AND DISCUSSION

Modified Impregnation (M_{Im}) Strategy. The interaction of chloride anions with Au nanoparticles and the resulting (usually negative) effect on the catalytic activity of these materials remains one of the most intriguing aspects of the wet chemical synthesis of Au-based catalysts.[5,35−38] Previous reports indicate a correlation between the decrease in the catalytic activity and the presence of chloride ions in the catalyst, and most studies have been directed at removing these chloride ions, with the aim of making the catalysts more active.[39] Some previous attempts to use excess chloride ions have been reported, but only limited success was achieved using an incipient wetness method, and efforts to use excess chloride ions in the C_{Im} method proved unsuccessful.[28,40]

Against this background we have developed a modified impregnation method (denoted M_{Im}) whereby an excess of Cl^- ions are utilized to generate highly active and stable supported gold−palladium nanoparticles. While synthesizing the bimetallic catalysts from their $HAuCl_4$ and $PdCl_2$ precursors, we introduced an excess of Cl^- ions by adding aqueous HCl into the wet impregnation medium. It is considered that the abundance of Cl^- ions present in the aqueous medium facilitates the formation of the $AuCl_4^-$ species for the gold precursor and, most importantly, the $PdCl_4^{2-}$ species for the palladium precursor. It is further proposed that the coexistence of these two species in the aqueous medium facilitates the formation of a more homogeneous mixture of metal ions, thereby enabling improved dispersion during the impregnation stage. In the absence of excess of chloride ions, (*i.e.*, the C_{Im} route) a $[Au(OH)_x(Cl)_{4-x}]^-$ gold precursor forms (where x is always >1) and the palladium precursor tends to form insoluble salts, as it is well-known that $PdCl_2$ is only sparingly soluble in water. The presence of this combination of species poses a problem for the conventional C_{Im} method, and leads to ineffective adsorption onto the support which can result in the formation of some very big metallic particles which are essentially inactive as catalysts.

Crucially, it should be noted that the as-synthesized and dried material prepared by our M_{Im} route then needs to be heated at 400 °C in a stream of 5% H_2 in Ar in order to observe the best catalytic activity. This gas-phase reduction step serves to substantially decrease the number of chloride ions present in the final catalyst, as demonstrated by the ICP−OES quantification of the residual chloride ions concentration in the as-synthesized and dried M_{Im} materials compared with the reduced material [Supporting Information; Tables ST1,ST2].

Catalytic Performance of M_{Im} *versus* C_{Im} Materials. *Direct Synthesis of Hydrogen Peroxide.* We have used the direct synthesis of hydrogen peroxide as one of two test reactions to demonstrate the efficacy of this new M_{Im} preparation method. The heterogeneously catalyzed direct synthesis of hydrogen peroxide from hydrogen and oxygen presents an attractive alternative to the current industrial anthraquinone process.[13] A number of studies have shown that the addition of Au into a Pd catalyst results in much higher selectivity toward H_2O_2 without the need for chemical promoters in the reaction medium, particularly when the material is synthesized by the C_{Im} route.[13,19] In particular, AuPd/TiO_2 catalysts were very selective for H_2O_2 synthesis,[19] and hence the AuPd catalysts prepared by our modified impregnation method were evaluated for this

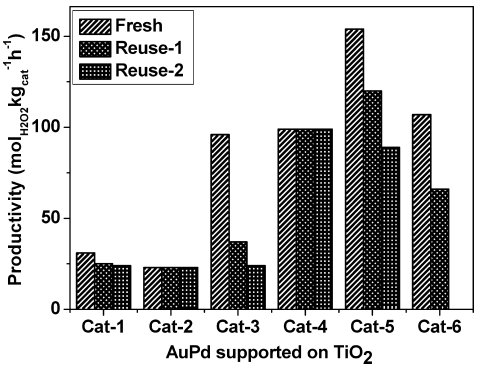

Figure 1. Comparison of activity and reusability data for the direct synthesis of hydrogen peroxide for supported 0.5% Au + 0.5%Pd/TiO_2 catalysts prepared by sol-immobilization S_{Im} (Cat-1), conventional impregnation C_{Im} (Cat-2), and modified impregnation M_{Im} methodologies (Cat-3−6). The modified impregnation catalysts tested are standard M_{Im} dried only (Cat-3), reduced in 5% H/Ar at 400 °C/4 h (Cat-4) [hydrogen conversion and selectivity for this catalyst are 18% and 70% respectively], M_{Im} prepared by NaCl excess (Cat-5), and M_{Im} prepared by 2 M HCl (Cat-6). Reaction conditions: 5% H_2/CO_2 and 25% O_2/CO_2, 50% H_2/O_2 at 3.7 MPa, MeOH (5.6 g), H_2O (2.9 g), catalyst (0.01 g), 2 °C, 1200 rpm, 30 min.

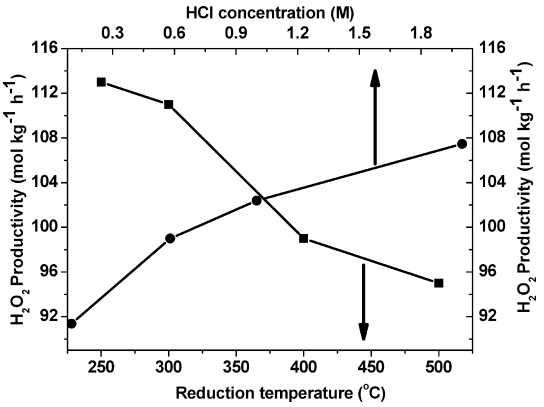

Figure 2. Effect of the amount of "excess" HCl added during the synthesis of the 0.5%Au + 0.5%Pd/TiO_2 (M_{Im}) catalyst on the resultant activity for the direct synthesis of hydrogen peroxide. In addition, the effect of the gas phase reduction temperature employed during the synthesis of a standard 0.5%Au−0.5%Pd/TiO_2 (M_{Im}) catalyst (using 0.58 M HCl) on the resultant activity for the direct synthesis of hydrogen peroxide is also plotted. Reaction conditions: 5% H_2/CO_2 and 25% O_2/CO_2, 50% H_2/O_2 at 3.7 MPa, MeOH (5.6 g), H_2O (2.9 g), catalyst (0.01 g), 2 °C, 1200 rpm, 30 min. Key: (●) H_2O_2 productivity *vs* HCl concentration; (■) H_2O_2 productivity *vs* reduction temperature.

particular reaction. We have previously shown that a 2.5 wt % Au + 2.5 wt % Pd/TiO_2 catalyst, calcined at 400 °C, has a productivity of 64 mol H_2O_2 kg cat^{-1} h^{-1}.[41] To ascertain whether a lower Au and Pd loading could be utilized for the direct synthesis of hydrogen peroxide, a series of catalyst materials were prepared with a 1 wt % total metal loading (0.5 wt % Au + 0.5 wt % Pd) by the S_{Im}, C_{Im} and M_{Im} routes, and their productivities were then compared under standard reaction conditions as shown in Figure 1.[41] In addition, the M_{Im} catalysts show a synergy between the Au and Pd components (Supporting Information, Table ST3) as has been observed with C_{Im} catalysts.[19,31] The C_{Im} catalyst after calcination, although less active (23 mol H_2O_2 kg cat^{-1} h^{-1}) compared to the material prepared by the sol-immobilization method (32 mol H_2O_2 kg cat^{-1} h^{-1}), is found to be stable for several reuse cycles, whereas the S_{Im} catalysts tend to lose their activity upon reuse.[42] However, we found that the AuPd M_{Im} catalyst was nearly four times more effective than the AuPd C_{Im} catalyst, with an activity of 99 mol H_2O_2 kg cat^{-1} h^{-1}. This catalyst is considerably more active than the previous best and stable AuPd/TiO_2 catalyst[41] (64 mol H_2O_2 kg cat^{-1} h^{-1}) prepared by the C_{Im} route, even though the new M_{Im} catalysts contains five times less metal (see Supporting Information, Table ST4). Interestingly the initial rates for the C_{Im} and M_{Im} catalysts are identical (Supporting Information, Figure S1). It is at longer reaction times, which are essential for H_2O_2 synthesis, that the differences are apparent (Figure S1) and the M_{Im} catalysts significantly out-perform the C_{Im} materials.

A crucial factor to consider in evaluating catalytic materials is their reusability. To determine their reusability, a small portion of each catalyst was evaluated for H_2O_2 synthesis, recovered by filtration, and then re-evaluated under standard reaction conditions. This used material was then recovered a second time by filtration, and evaluated for a third time under standard reaction conditions (Figure 1). While the calcined C_{Im} catalyst showed a stable activity (Figure 1), unfortunately the dried-only M_{Im} catalyst did not maintain a high activity during the second use, displaying a decrease in productivity from 99 to 40 mol H_2O_2 kg cat^{-1} h^{-1}. However, when the dried M_{Im} catalyst was reduced in 5% H_2 in Ar at 400 °C, the 99 mol H_2O_2 kg cat^{-1} h^{-1} activity level was maintained for three successive usage cycles. This demonstrates that the gas phase reduction procedure in 5 % H_2/Ar at 400 °C is essential for increasing the stability of the M_{Im} catalyst without compromising the catalytic activity.

The standard 0.5 wt % Au + 0.5 wt % Pd/TiO_2 M_{Im} catalyst reported above was prepared in a medium containing an "excess of chloride ions" generated by the addition of 0.58 M HCl to the catalyst synthesis medium during the impregnation stage. To optimize the amount of "excess" chloride ions required to obtain the most active catalyst, a systematic series of samples were prepared in which a range of HCl concentrations (*i.e.*, 0.1, 0.58, 1, and 2 M) were added to the catalyst synthesis medium. These catalysts were then compared for their hydrogen peroxide productivity, as shown in Figure 2, and it was found that increasing the chloride ion concentration increases the activity of the catalyst. However, although the catalysts prepared with 1 and 2 M HCl solutions show a higher H_2O_2 productivity, they are not stable for reuse, whereas the "standard M_{Im}" catalyst prepared with a 0.58 M HCl solution is stable for reuse (Figure 1, Cat-6).

TABLE 1. Effect on the Hydrogen Peroxide Productivity[a] of Using Different Palladium Precursors in the Synthesis of the 0.5%Au + 0.5%Pd/TiO_2 Catalyst

palladium precursor	productivity ($mol_{H_2O_2}\ kg_{cat}^{-1}\ h^{-1}$)	hydrogenation activity ($mol_{H_2O_2}\ kg_{cat}^{-1}\ h^{-1}$)
$PdCl_2$	99	230
Na_2PdCl_4	87	136
$Pd(NO_3)_2$	100	583
$PdBr_2$[b]	59	173
$PdCl_2$[c]	32	nd[d]

[a] Reaction conditions: 5% H_2/CO_2 and 25% O_2/CO_2, 50% H_2/O_2 at 3.7 MPa, MeOH (5.6 g), H_2O (2.9 g), catalyst (0.01 g), 2 °C, 1200 rpm, 30 min. [b] Gold precursor is $AuBr_3$ in the presence of an excess of HBr. [c] This catalyst was prepared in an aqueous solution of 0.19 M H_3PO_4. [d] nd = Not determined.

It is possible that the role of the excess Cl^- is to permit the formation of the most effective $[AuCl_4]^-$ and $[PdCl_4]^{2-}$ precursor species in the aqueous medium. However, it is also plausible that the presence of excess Cl^- could improve the dispersion of the metal ions during the adsorption stage by competitive adsorption over the support. A similar effect has been observed previously during the preparation of monometallic gold catalysts, but here we demonstrate that this "excess-anion" effect is very effective for the bimetallic gold−palladium catalysts.[28] To investigate the hypothesis that the formation of a palladate precursor is essential to enable the most active catalyst to be formed, a range of palladium precursors were tried for the synthesis of 0.5 wt %Au 0.5 wt %Pd/TiO_2 catalysts and the results are presented in Table 1. A catalyst prepared by dissolving Na_2PdCl_4 in water gave a comparable activity (87 mol H_2O_2 kg cat^{-1} h^{-1}) to that of the standard M_{Im} catalyst, which gave an activity of 99 mol H_2O_2 kg cat^{-1} h^{-1}. The slightly higher activity of the standard M_{Im} catalyst could be attributed to the effect of the additional chloride ions present in the aqueous medium as dilute HCl, which were not present for the catalyst prepared using Na_2PdCl_4.

To investigate further the role of the chloride ions, an equimolar aqueous sodium chloride solution was used during the M_{Im} catalyst synthesis in place of the aqueous HCl. Here, NaCl provided the chloride ions in a neutral pH environment. When this catalyst was tested for the direct synthesis of hydrogen peroxide it was found to be even better than the standard M_{Im} catalyst prepared using 0.58 M HCl, displaying a productivity of 154 mol H_2O_2 kg cat^{-1} h^{-1}. This demonstrates that the excess of chloride ions are indeed associated with the higher activity displayed by the catalysts prepared by M_{Im}. Unfortunately the NaCl-derived material deactivated upon reuse (see Figure 1) even after the H_2 reduction treatment at 400 °C which afforded stability to the M_{Im} catalyst prepared using HCl.

A catalyst was also synthesized in the presence of 0.29 M H_2SO_4 instead of 0.58 M HCl in order to study the role of the pH of the synthesis medium on the resultant catalytic activity. This catalyst was found to be the least reactive among all the catalysts screened, having an activity of only 16 mol H_2O_2 kg cat^{-1} h^{-1}. To further eliminate the effect of pH, the same catalyst was prepared in an aqueous solution of 0.19 M H_3PO_4, and the activity for this catalyst was found to be only 32 mol H_2O_2 kg cat^{-1} h^{-1} (see final entry in Table 1). From this result, it is clear that the enhancement of catalytic activity for the M_{Im} catalysts is not only because of pH of the synthesis medium. A 0.5 wt % Au + 0.5 wt %Pd/TiO_2 catalyst was also prepared using $AuBr_3$ and $PdBr_2$ as the metal precursors, and an "excess" of Br^- anions was provided by adding a 0.5 M aqueous HBr solution. The hydrogen peroxide productivity of the Br^- excess sample was 59 mol H_2O_2 kg cat^{-1} h^{-1}(Table 1) which is inferior to that found for materials prepared with excess Cl^- anions. It therefore appears that this "excess anion" strategy is only effective when using chloride ions.

Another crucially important stage in the preparation of the catalysts by the M_{Im} method is the gas-phase reduction in 5% H_2/Ar. Recently Kaneda *et al.* reported that the reduction temperature plays a crucial role in the resultant activity of supported metal catalysts.[43] To investigate this parameter for the current method, the 'as-synthesized' and dried 0.5 wt % Au + 0.5 wt % Pd/TiO_2 M_{Im} catalyst was reduced at a series of different temperatures (namely, 250, 300, and 500 °C) in addition to the standard temperature of 400 °C. The resultant materials were evaluated for their hydrogen peroxide productivity as shown in Figure 2. The productivity was found to gradually decrease with increasing reduction temperature, possibly due to the formation of larger particles at the expense of the most active small particles at the higher reduction temperatures. However, the high temperature gas-phase reduction step is crucial to make these catalysts stable for reuse, as evidenced from the data presented in Figure 1. Thus a compromise was made by performing the reduction treatment at 400 °C, as this imparted a sufficient degree of catalyst stability without significantly reducing the catalyst productivity.

A number of different AuPd catalysts were prepared on alternative supports (*e.g.*, CeO_2, MgO, SiO_2, C) by this M_{Im} method, and tested for the direct synthesis of H_2O_2 (see Supporting Information, Table ST4). When TiO_2, MgO, and SiO_2 were used as supports, the M_{Im} catalysts were substantially more active than the corresponding C_{Im} catalysts. At first sight Table ST4 seems to suggest that the productivity was lower for the CeO_2 and C supported M_{Im} materials. However, it should be noted here that all the C_{Im} catalysts in this particular set of samples had *five* times more metal loading than the corresponding M_{Im} catalysts, which implies that on all

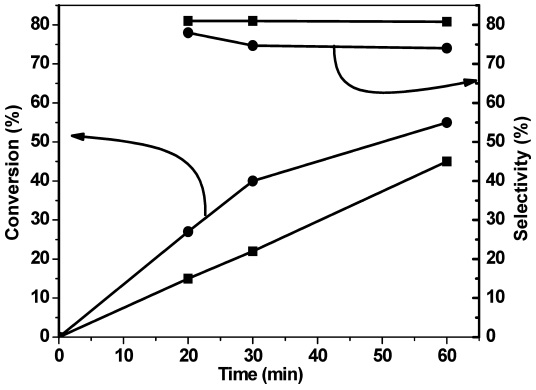

Figure 3. Comparison of the catalytic activities of 0.5%Au + 0.5%Pd/TiO_2 catalysts prepared by M_{Im} and C_{Im} for the solvent-free aerobic oxidation of benzyl alcohol in a glass stirred batch reactor. Reaction conditions: benzyl alcohol = 2 g, 0.02 g of catalyst, T = 120 °C, p_{O_2} = 1 bar (relative), stirring rate 1000 rpm. Key: (■) C_{Im} catalyst (showing both benzyl alcohol conversion and benzaldehyde selectivity); (●) M_{Im} catalyst (showing both benzyl alcohol conversion and benzaldehyde selectivity).

the support materials tested, the M_{Im} catalysts are to varying degrees superior to the C_{Im} catalysts.

Benzyl Alcohol Oxidation under Solvent-free Conditions. A second important class of reaction that can be effectively catalyzed by supported gold−palladium nanoparticles is the selective oxidation of alcohols.[19] In view of this fact, we have also investigated the catalytic oxidation of benzyl alcohol under solvent-free conditions at 120 °C to compare the activities of 0.5 wt %Au + 0.5 wt %Pd/TiO_2 catalysts prepared by both C_{Im} and M_{Im} routes (see Figure 3). While the M_{Im} catalyst is more active than the C_{Im} catalyst for benzyl alcohol oxidation, the selectivity for benzaldehyde (the desired product) is slightly lower for the M_{Im} catalyst. This suggests that the M_{Im} catalyst is more active also for the competing disproportionation reaction which results in the formation of an equimolar mixture of toluene and benzaldehyde.[44,45] The enhanced catalytic activity of the M_{Im} catalyst is considered to be due an optimized nanostructure compared to the corresponding C_{Im} catalysts. We are currently developing ways to improve the selectivity toward benzaldehyde for the M_{Im} catalysts without compromising the activity, and are also investigating the selective oxidation of other alcohol substrates.

Catalyst Characterization. *STEM Comparison of M_{Im} and C_{Im} Materials.* Detailed high angle annular dark field (HAADF) imaging and STEM-XEDS studies were carried out to compare the morphologies of 0.5 wt %Au + 0.5 wt %Pd/TiO_2 catalysts prepared by the C_{Im} and M_{Im} (0.58 M HCl) preparation routes under three distinct conditions *viz,* dried-only, calcined at 400 °C, reduced in 5%H_2/Ar. Representative data for these C_{Im} and M_{Im} samples are shown in Figure 4 and 5, respectively. The dried-only C_{Im} (Figure 4a,b) and dried-only M_{Im} (Figure 5a,b) materials show rather similar morphologies with numerous 1−2 nm Pd-rich clusters and

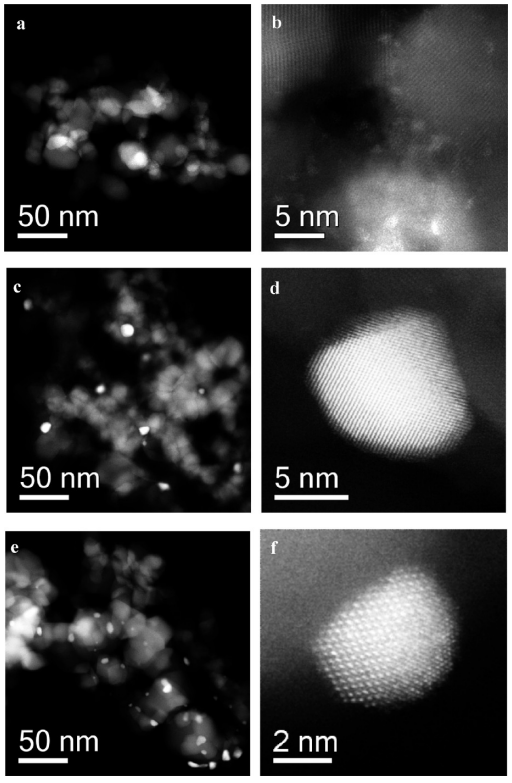

Figure 4. HAADF-STEM images of 0.5%Au + 0.5%Pd/TiO_2 catalysts prepared by the C_{Im} method. (a,b) Dried only at 120 °C; (c,d) calcined in air at 400 °C; (e,f) reduced in 5%H_2/Ar at 400 °C.

atomically dispersed species as well as occasional large (micrometer scale) gold-rich particles which originate from a poor dispersion of the gold component. After calcination in air at 400 °C (C_{Im}, Figure 4c,d; M_{Im}, Figure 5c,d) some sintering occurs and both materials show 5−10 nm particles which have a distinct Au-rich core and Pd-rich shell morphology. In addition, there are still numerous Pd-rich clusters and atomically dispersed species remaining on the TiO_2 supports. If the C_{Im} and M_{Im} dried-only materials are subjected to a 400 °C reducing (5%H_2/Ar) treatment instead of calcination (C_{Im}, Figure 4e,f; M_{Im}, Figure 5e,f) then all the clusters and atomically dispersed species are now absent and have been efficiently subsumed into the larger random alloy particles. However, the reduced C_{Im} and M_{Im} materials do show a distinct difference in AuPd particle size distribution, with mean values of 4.7 and 2.9 nm, respectively. All these catalysts: C_{Im} calcined, C_{Im} reduced, M_{Im} calcined, and M_{Im} reduced were evaluated for the direct synthesis of hydrogen peroxide and the results are presented in the Supporting Information (Table ST 5). For both C_{Im} and M_{Im} catalysts, the reduced materials have superior catalytic activity compared to their calcined analogues: C_{Im} (calcined) and C_{Im} (reduced) catalysts have activities of 23 and 68 mol H_2O_2 kg cat^{-1} h^{-1}, respectively, M_{Im} (calcined) and M_{Im} (reduced) catalysts have activities 36 and 99 mol H_2O_2 kg cat^{-1} h^{-1}, respectively.

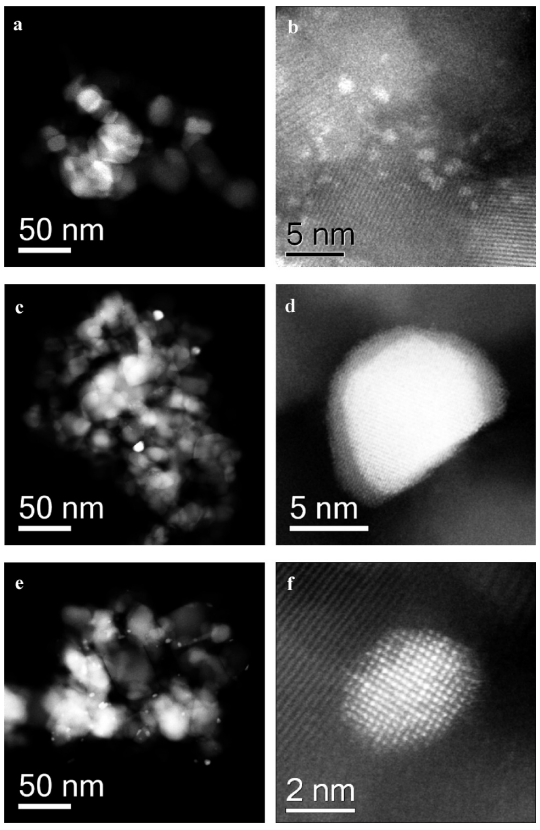

Figure 5. HAADF images of 0.5%Au + 0.5%Pd/TiO_2 catalysts prepared by the M_{Im} method with 0.58 M HCl. (a,b) dried only at 120 °C; (c,d) calcined in air at 400 °C; (e,f) reduced in 5%H_2/Ar at 400 °C.

The difference in catalytic activity between the M_{Im} and C_{Im} catalysts could be because of the "excess" anion effect where the difference between "calcined" and "reduced" catalysts within the set could be because of the structural differences of the nanoalloys. This suggests that the random alloy structures are catalytically more active compared to the core−shell morphologies.

STEM Analysis of the M_{Im} Materials before and after Use. Using aberration corrected STEM, the dried only 0.5 wt %Au + 0.5 wt %Pd/TiO_2 M_{Im} material, and the 0.5 wt %Au + 0.5 wt %Pd/TiO_2 M_{Im} catalyst reduced at 400 °C in H_2/Ar, were studied both in the fresh and used states. Figure 6 panels a and b show representative HAADF images of the nanostructure of the unused, dried 0.5 wt %Au 0.5 wt %Pd/TiO_2 M_{Im} catalyst. There are two types of metal species present in these images, namely (i) 1−2 nm metallic clusters and (ii) isolated Au or Pd atoms. After use (Figures 6c,d), neither 1−2 nm clusters nor individual metal atoms could be found on the support, implying that these metal species were unstable and have leached from the catalyst during the catalytic testing. This was confirmed by AAS/ICP analysis (Supporting Information, Table ST1) where a decrease of ~60 to 70% in total Au and Pd content was found after use. Hence, it is the loss of the active metal component that is responsible for the observed deactivation of the dried-only material.

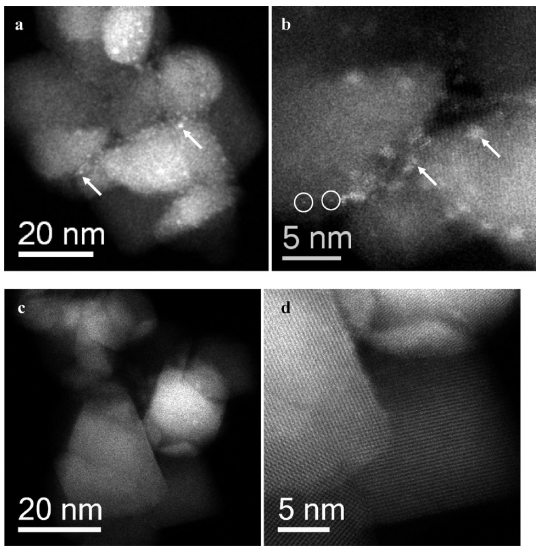

Figure 6. (a,b) STEM-HAADF images of the unused, dried only 0.5%Au + 0.5%Pd/TiO_2 prepared by the M_{Im} route (0.58 M HCl); 1−2 nm rafts (arrowed in white) and isolated atoms (circled in white) are clearly visible in the fresh sample. (c,d) STEM-HAADF images of the corresponding material after one usage cycle in which all the supported Au species have been lost.

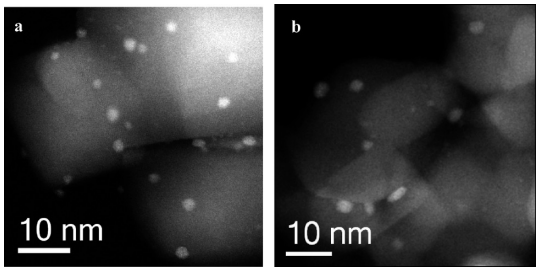

Figure 7. STEM-HAADF images of 0.5%Au + 0.5%Pd/TiO_2 prepared by the M_{Im} route (0.58 M HCl) that were reduced in H_2/Ar at 400 °C: (a) fresh and (b) after one usage cycle.

Representative STEM-HAADF images of the 0.5 wt %Au + 0.5 wt %Pd/TiO_2 material prepared by M_{Im} (0.58 M HCl) and reduced at 400 °C in an H_2/Ar mixture, in the fresh and used states, are shown in Figure 7 panels a and b, respectively. In both cases, a homogeneous dispersion of metal nanoparticles were noted that had a 2−5 nm size range. Furthermore, no obvious metal leaching (Supporting Information, Tables ST1,ST2) or particle coarsening was noticed in the used samples as compared to the fresh ones. Interestingly, no 1−2 nm clusters and very few individual metal atoms were noted in either of these reduced samples, implying that these species had been incorporated into the 2−5 nm particles by sintering during the 400 °C H_2/Ar reduction step. Compositional information from individual particles was also obtained by STEM-XEDS for these latter samples, as shown in Figure 8. X-ray signals were collected while scanning the electron beam over the entire particle, so the XEDS spectrum presented should be treated as an average composition over the entire

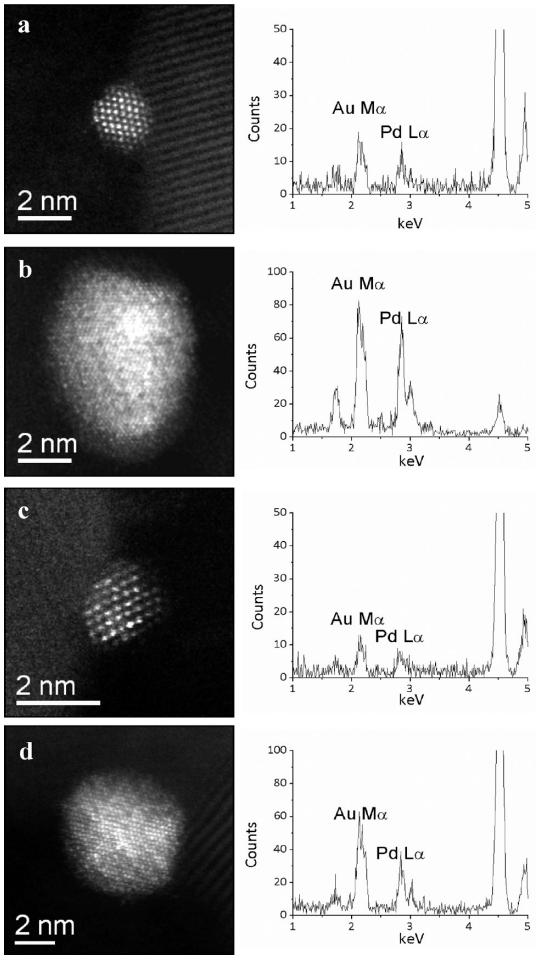

Figure 8. High magnification STEM-HAADF images and corresponding XEDS spectra from individual metal particles in the 0.5%Au + 0.5%Pd/TiO_2 samples prepared by M_{Im} (0.58 M HCl) and reduced at 400 °C in H_2/Ar: (a,b) data obtained from small (2 nm) and larger (6 nm) particles in the fresh sample; (c,d) data obtained from small (2 nm) and larger (7 nm) particles in the used sample.

particle. It was found that small (~2 nm) and larger (~6 nm) particles from the fresh (Figure 8a,b) and used samples (Figure 8c,d) are all AuPd alloys of relatively similar composition. Importantly, these alloyed particles show a higher catalytic activity than the corresponding "dried-only" catalysts and are totally reusable. Furthermore, based on the intensity ratios between the Au M_α and Pd L_α lines, there seems to be no significant size-dependent composition variation. This is quite a significant result as catalysts prepared by the sol-immobilization (S_{Im}) and conventional impregnation methods have previously been shown to display systematic composition variations with particle size. For S_{Im} catalysts, the larger particles were always Pd-rich, and the smaller ones were Au-rich.[42,46] For the conventional impregnation route, the situation is reversed, with the larger particles having been reported as being Au-rich, and the smaller ones being reported as Pd-rich.[47,48] These results clearly demonstrate that the modified impregnation route represents an effective new method for producing AuPd nanoparticles with a tight size distribution, along with minimal composition variation across this size range.

We were unable to measure the compositions of the ultrasmall 1−2 nm metallic clusters present in the dried-only M_{Im} samples simply because they were mobile under the electron beam and produced too little signal for meaningful XEDS analysis. Therefore the corresponding monometallic Au/TiO_2 and Pd/TiO_2 M_{Im} systems were studied by STEM-HAADF imaging in order to evaluate how the modified impregnation method affected the distribution of each metal component individually. It was found that the dried only Au/TiO_2 M_{Im} sample contains 1−2 nm Au clusters and individual Au atoms (Supporting Information, Figure S3a,b), while after reduction at 400 °C in H_2/Ar these species aggregated and formed nanoparticles which were 2−6 nm in diameter (Supporting Information, Figure S3c,d). The monometallic Pd/TiO_2 M_{Im} sample seemed to behave in a subtly different manner, in that 1−2 nm Pd rafts dominated with little evidence for individual Pd atoms (Supporting Information Figures S4a,b). After a reduction at 400 °C, 2−6 nm Pd nanoparticles were formed as expected (Supporting Information Figures S4c,d and Figure S5). From these studies on the two monometallic systems, we can infer that both Au and Pd can be finely dispersed into 1−2 nm clusters in the presence of excess Cl^- species. During reduction at 400 °C in H_2/Ar, where the residual Cl^- had been largely removed, the clusters sinter to form nanoparticles. Since the two metals were so well dispersed initially, the resultant alloy nanoparticles can be well controlled both in terms of size and composition.

STEM Analysis of M_{Im} Materials Prepared in the Presence of Different [Cl^-] Anion Concentrations. Detailed high angle annular dark-field (HAADF) imaging and STEM-XEDS studies have been carried out on a series of 0.5 wt %Au + 0.5 wt %Pd/TiO_2 catalysts prepared using different [Cl] concentrations (namely (i) 0 M HCl (*i.e.*, C_{Im}), (ii) M_{Im}−0.58 M HCl, and (iii) M_{Im}−2.0 M HCl). The results of these analyses are shown in Figures 9 and 10. All three samples in the dried-only state look very similar in HAADF-STEM mode (Figure 9a−c) displaying 1−2 nm clusters and atomically dispersed species. After reduction in 5%H_2/Ar, all three materials show larger AuPd alloy particles (Figure 9d−f) and a complete absence of clusters. Analysis of the particle size distributions from such micrographs (Figure 10a,c,e) show that the mean particle size and spread of particle size decreases with increasing [Cl] concentration (C_{Im} mean, 4.7 nm; M_{Im}−0.58 M HCl mean, 2.9 nm; M_{Im}−2.0 M HCl mean, 2.6 nm). Representative images and XEDS spectra from individual particles from these three specimens are shown in Figure 9 (C_{Im}, Figure 9g,j; M_{Im}−0.58 M HCl, Figure 9h,k; M_{Im}−2.0 M HCl, Figure 9 i,l). All the particles are largely random alloys in nature, but do show a

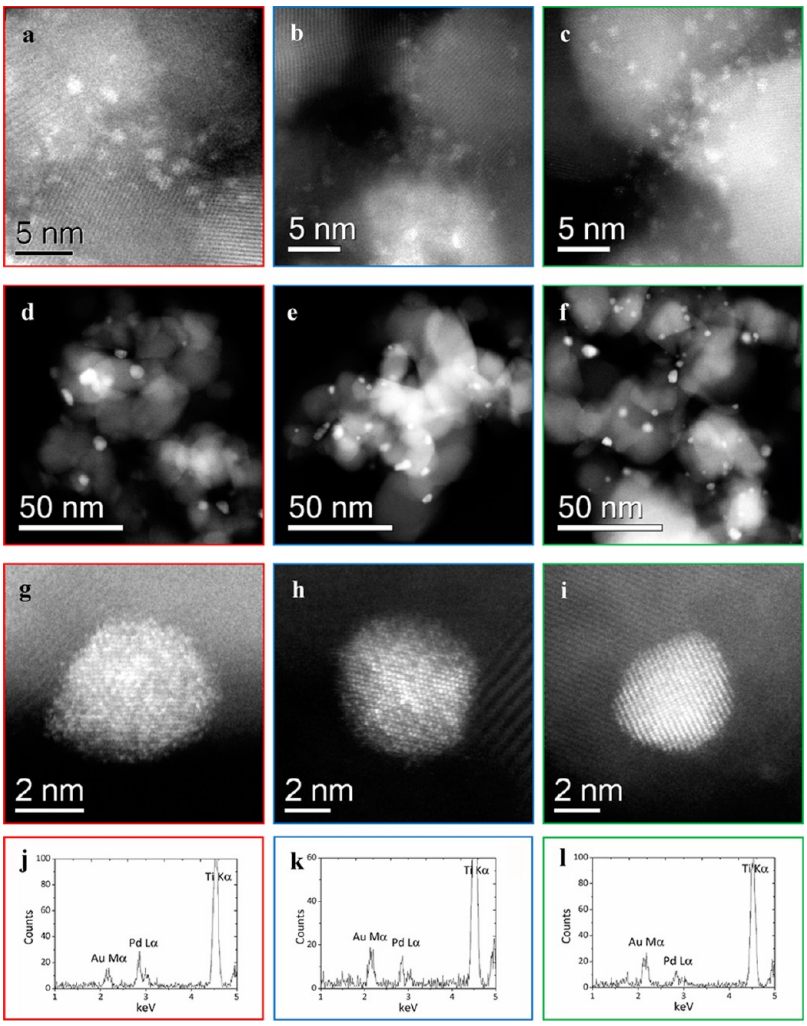

Figure 9. Images of 0.5%Au + 0.5%Pd/TiO_2 samples prepared with no HCl (*i.e.*, C_{lm}), red column; 0.58 M HCl (M_{lm}), blue column; and 2.0 M HCl (M_{lm}), green column: (a−c) HAADF images of dried only samples; (d−i) HAADF images of samples reduced in 5%H_2/Ar at 400 °C (j, k, l) XEDS spectra from the particles shown in panels g, h, and i, respectively, in which a systematic increase in Au content correlates with increasing HCl concentration used in the preparation.

systematic change in Pd:Au ratio with varying [Cl] concentration. A more statistically relevant analysis of composition with particle size for these three samples is presented in Figure 10b,d,f). It is clear that increasing the amount of excess [Cl] used in the M_{lm} preparation causes a definite increase in Au content within the AuPd alloy particle. This compositional variation trend can be rationalized by analyzing these samples by backscattered electron (BSE) imaging in an SEM to monitor the population of the larger scale (200 nm to 2.0 μm) Au particles (see Supporting Information, Figure S6). It is clear the C_{lm} material contains a significant population of poorly dispersed Au, but the effect of the excess Cl in the M_{lm} materials is to progressively disperse (*i.e.*, eventually eliminate) these large Au species. As this Au is no longer associated with large inactive particles, it can be incorporated in to the nm scale AuPd alloy particles, therefore increasing their mean gold content. Increasing the Au content in the particle improves the H_2O_2 productivity, but simultaneously decreases the catalyst reusability. The M_{lm} (2 M HCl) catalyst showed a decrease in productivity from 107 to 66 mol H_2O_2 kg cat^{-1} h^{-1} upon reuse. (Figure 2 for productivity and Figure 1 (Cat-6) for reusability). At this stage, the reason for this observed instability of the M_{lm} 2 M HCl catalyst is unknown, but detailed characterization of these fresh and reused materials are currently underway. However, this implies that the intermediate (0.58 M HCl) M_{lm} sample has a AuPd particle composition that is a good compromise for yielding a catalyst that simultaneously has a reasonable H_2O_2 productivity *and* effective reusability characteristics.

STEM Analysis of M_{lm} Materials Prepared Using Reagents Other than HCl. The modified impregnation samples prepared using NaCl and H_2SO_4 in place of HCl were also examined by STEM. These two samples, designated M_{lm}-NaCl and M_{lm}-H_2SO_4, respectively, were studied in the unused state after having been reduced at 400 °C in H_2/Ar. Representative HAADF images of the M_{lm}-NaCl and M_{lm}-H_2SO_4 samples (Supporting Information, Figure S7 panels

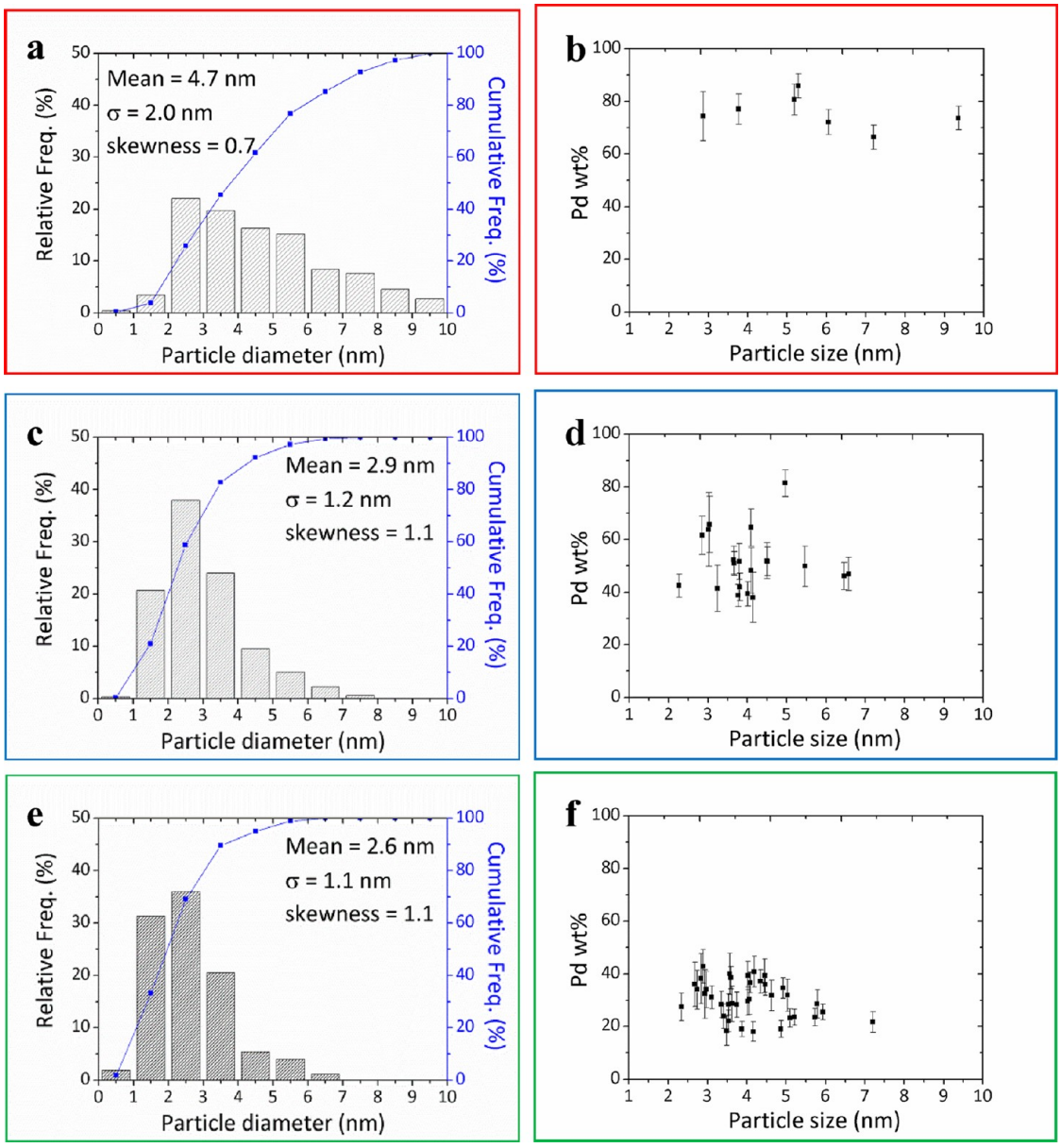

Figure 10. Particle size distributions for 0.5%Au + 0.5%Pd/TiO_2 samples prepared with (a) no HCl (*i.e.*, C_{Im}), (c) 0.58 M HCl (M_{Im}), and (e) 2.0 M HCl (M_{Im}); particle size/composition diagrams for AuPd/TiO_2 samples prepared with (b) no HCl (*i.e.*, C_{Im}), (d) 0.58 M HCl (M_{Im}), and (f) 2.0 M HCl (M_{Im}). All samples have been reduced in 5%H_2/Ar at 400 °C. Note that increasing the HCl concentration in the preparation causes a progressive increase in the gold content within the alloy particles.

a and b, respectively) show them to have very similar 2−6 nm particle size distributions. Figure S8 (Supporting Information) shows representative atomic resolution HAADF images of some small (2 nm) and large (5 nm) particles along with their corresponding XEDS spectra for the M_{Im}-NaCl sample. It is clear that the metal particles in M_{Im}-NaCl are all homogeneous Au−Pd alloys, which is a characteristic that it has in common with the M_{Im}-HCl derived sample, and consistent with the fact that both these samples show excellent catalytic activity. By way of contrast, similar HAADF images and XEDS spectra of small (2 nm) and larger (6 nm) particles from the M_{Im}-H_2SO_4 sample are presented in Figure S9 (Supporting Information). It is clear that the metal particles in this case are comprised almost entirely of Au and any Pd, if present at all, is below the detectability limit of the XEDS technique. This finding correlates very well with the poor catalytic activity displayed by the M_{Im}-H_2SO_4 sample, since AuPd alloy particles are not generated. The mystery of the Pd location in the M_{Im}-H_2SO_4 sample was easily resolved by examining the M_{Im}-H_2SO_4 material at lower magnification in the SEM, where occasional micrometer-scale particles of $PdSO_4$ were observed (Supporting Information, Figure S10).

XPS Characterization of M_{Im} and C_{Im} Materials. The titania-supported catalysts prepared by the M_{Im} route, using different excess anions, and by the C_{Im} route were analyzed by X-ray photoelectron spectroscopy (XPS). Quantified data showing derived surface

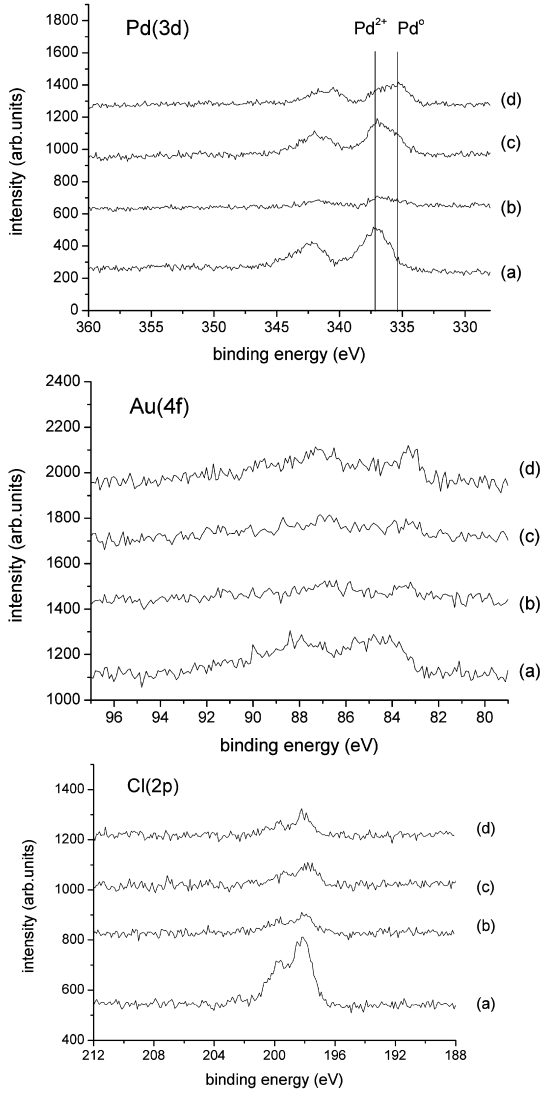

Figure 11. Pd(3d), Au(4f), and Cl(2p) spectra for 0.5%Au + 0.5%Pd/TiO_2 samples prepared by conventional impregnation (C_{Im}): (a) dried sample; (b) catalyst (a) after being used for H_2O_2 synthesis; (c) catalyst (a) after calcination in air at 400 °C; (d) catalyst (c) after use for H_2O_2 synthesis.

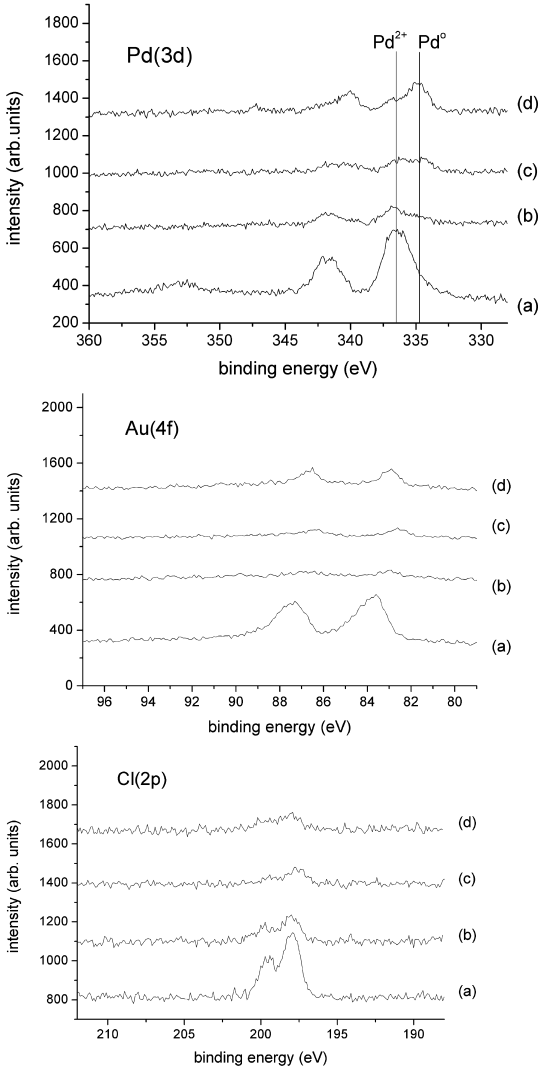

Figure 12. Pd(3d), Au(4f), and Cl(2p) spectra for 0.5%Au + 0.5%Pd/TiO_2 samples prepared by modified impregnation (M_{Im}) using excess HCl: (a) dried sample; (b) catalyst (a) after being used for H_2O_2 synthesis; (c) catalyst a after heating in H_2/Ar at 400 °C; (d) catalyst (c) after use for H_2O_2 synthesis.

compositions (atom %) and corrected Pd/Au ratios are shown in Table ST6 (Supporting Information), and detailed spectra for the C_{Im} and M_{Im} (0.58 M HCl) samples are presented in Figures 11 and 12, respectively. We have analyzed the dried and calcined/reduced catalysts, both fresh and after use for hydrogen peroxide synthesis. The behavior of the C_{Im} samples has been reported previously;[41] calcination of the dried C_{Im} sample leads to a significant increase in the Pd:Au ratio due to the formation of particles with a Pd-rich shell/Au-rich core morphology. Furthermore, use of the dried-only C_{Im} catalyst for H_2O_2 synthesis results in significant leaching, as reflected in the decrease in the [Au]+[Pd] value, whereas the calcined sample was stable. In marked contrast, the M_{Im} samples derived from HCl or NaCl show no strong evidence for core−shell formation on reduction at 400 °C (for a random alloy the expected Pd:Au ratio is 1.9:1), but in common with the C_{Im} materials do show leaching after use for the dried-only catalyst, but not for the 400 °C reduced samples. The C_{Im} and M_{Im}−HCl and M_{Im}-NaCl catalysts exhibit similar Cl surface concentrations for the dried materials, and only the latter shows no significant decrease after heat treatment. Interestingly, both oxidative (C_{Im}) and reductive (M_{Im}-HCl) heat treatments are able to decrease the residual [Cl] concentration. For all dried-only samples the [Cl] concentration decreases significantly after use for H_2O_2 synthesis.

The low Pd signals for the $M_{Im}(H_2SO_4)$ samples are in keeping with the results of the STEM-XEDS studies which identified large microscopic $PdSO_4$ particles, where most of the Pd atoms would be not detected by XPS, since the mean free path for photoelectrons is orders of magnitude smaller than the $PdSO_4$ particle size.

Quantified XPS data, together with the corrected Pd:Au ratios for M_{Im} samples prepared with varying HCl concentration, are shown in Table ST7 (Supporting Information). After reduction in H_2/Ar at 400 °C we observe only minor differences between the Pd/Au ratios for the 0.1M, 0.58 and 2 M materials. This is contrasts with the STEM observation that large Au particles are not present in the 2 M catalyst, the gold having been dispersed and incorporated into Pd−Au alloy nanoparticles. Although increased dispersion of the gold will lead to an increase in the Au(4f) signal intensity for those gold atoms, which might be reflected by a decrease in the Pd/Au ratio, XPS provides information averaged over a relatively large area and in this case is dominated by the AuPd nanoparticles. For all three preparations, the [Cl] concentration decreases significantly after reduction. The observed Au($4f_{7/2}$) binding energies, 82.6−83.1 eV, are lower than the expected bulk value of 84.0 eV. Some groups have related this negative shift to the change in electronic structure as a function of cluster size,[49,50] while other groups attribute it to (i) electron transfer from the support to the nanoparticles,[51,54] (ii) an initial state effect resulting from H_2 pretreatment,[52] or (iii) charge transfer from Pd to Au, increasing the *s*-state occupancy for Au and indicating alloy formation.[53] Clearly, based on the STEM results and the sample preparation, both of the latter two explanations could be applicable here. The Pd(3d) spectra in Figure 12 for a M_{Im} (0.58 M HCl) catalyst show that after reduction in H_2/Ar at 400 °C there is an increase in the intensity of the Pd(0) component relative to the Pd(II) component. There are no corresponding changes in the XRD traces (Supporting Information, Figure S11), consistent with this reduced layer being confined to the surface region and detectible by XPS (a surface sensitive technique) but not XRD (a bulk technique).

The measured Pd($3d_{5/2}$) binding energies lie in the range 336.0 ± 0.2 eV, somewhat lower than what we frequently observe for Pd^{2+} in Pd and Pd−Au nanoclusters, at around 336.5−337 eV.[47] In the light of the STEM results we consider this energy to be indicative of two possibilities: (i) particle-size effects, wherein the Pd core-hole screening during photoemission results in a higher binding energy for small particles[55] or (ii) $Pd^{\delta+}$ formation through charge transfer with adsorbed Cl,[56] although whether this Cl is adsorbed on the Pd itself, or neighboring sites is inconclusive from the XPS data alone. This latter point is in some agreement with Shen et al.[57] who reported similar Pd binding energies for Cl-containing catalysts, and suggests the Pd has a more positive valency resulting in a more stable Pd surface structure than the corresponding halide-free system.

CONCLUSIONS

A "stabilizer-free", modified impregnation methodology has been developed for preparing supported gold−palladium nanoalloy catalysts. The impregnation medium in our method contains a large excess of anionic ligands, namely Cl^-, which helps to improve the dispersion of the Au species in particular. The reduction treatment at 400 °C in a 5%H_2/Ar atmosphere is effective for removing the excess Cl^- from the catalyst, as well as efficiently "sweeping-up" the very highly dispersed, predominantly Pd-rich species, and aiding their efficient incorporation into the 2−5 nm AuPd alloy nanoparticles. Catalysts prepared by the M_{Im} method are found to be four times more active for the direct synthesis of hydrogen peroxide from H_2 and O_2 than those made by C_{Im} and S_{Im} methods. They are also more active for the solvent-free oxidation of benzyl alcohol, although some loss of specificity to the desired benzaldehyde product was noted. The metal nanoparticles in these M_{Im} materials have a tight distribution of particle sizes ranging from 2 to 6 nm with only very occasional very large particles, that is, their size range is much better controlled than the C_{Im} materials, and they are more akin in this respect to S_{Im} derived catalysts. Furthermore the bimetallic alloy composition is relatively invariant from particle-to-particle in these M_{Im} materials, in contrast to the C_{Im} and S_{Im} materials where systematic particle size/composition variations have previously been noted. In addition, we have found that the Au:Pd ratio of the alloy particles can to some extent be controlled by varying the concentration of excess [Cl^-] anions employed in the M_{Im} process. In summary, our new M_{Im} route permits the generation of a catalyst which has a small average particle size, an optimized random alloy composition, and improved compositional uniformity from particle-to-particle. This new preparation protocol provides the both the academic research community and the industrial community, with a very convenient and reproducible methodology for preparing supported Au−Pd nanoalloy catalysts with high activity and stability without using any exotic ligands or stabilizers, while at the same time not compromising their catalytic activity.

EXPERIMENTAL SECTION:

Catalyst Preparation. *Modified Impregnation (M_{Im}).* $HAuCl_4 \cdot 3H_2O$ (Sigma Aldrich) was used as a gold precursor and was dissolved in deionized water to form a solution with a gold concentration of 8.9 mg/mL. The $PdCl_2$ (Sigma Aldrich) salt was dissolved in a 0.58 M aqueous HCl solution (conc HCl, diluted using the requisite amount of deionized water) with gentle warming and vigorous stirring to form a solution with a Pd

concentration of 6 mg/mL. This solution was cooled and used as the palladium precursor. In a typical synthesis run, the requisite amount of gold solution and palladium solution were charged into a clean 50 mL round-bottom flask fitted with a magnetic stirrer bar. The volume of the solution was adjusted using deionized water to a total volume of 16 mL. The flask was then immersed into an oil bath sitting on a magnetic stirrer hot plate. The solution was stirred vigorously at 1000 rpm and the temperature of the oil bath was raised from 27 to 60 °C over a period of 10 min. At 60 °C, 1.98 g of the metal oxide support material [TiO_2 (Degussa Evonik P25), C (Darco G60, Sigma Aldrich), CeO_2 (<5micrometer, Sigma Aldrich), SiO_2 (Grace, Johnson Matthey), MgO (BDH)] was added slowly over a period of 8−10 min with constant stirring. After the completion of addition of the support material, the slurry was stirred at 60 °C for an additional 15 min. Following this, the temperature of the oil bath was raised to 95 °C, and the slurry was stirred at that temperature for a further 16 h until all the water evaporated leaving a dry solid. Subsequently the solid powder was transferred into a mortar and pestle and was ground thoroughly to form a uniform mixture. This was stored and designated as a "dried-only" sample. A 400 mg portion of the uncalcined sample was transferred and spread out over a glass calcination boat (30 cm in length). This boat was then put inside a calcination furnace fitted with an inlet and outlet valve. The temperature of the furnace was raised from 30 to 400 °C at a heating rate of 10 K/min under a steady flow of 5%H_2 in Ar. The sample was reduced at 400 °C for 4 h under a steady flow of 5% H_2 in Ar. Finally, the furnace was cooled and this "reduced" sample was used as the M_{Im} catalyst.

Sol Immobilization (S_{Im}). The S_{Im} catalysts were prepared using exactly the same procedure reported by us previously elsewhere.[44,45] In a typical catalyst synthesis (0.5%Au-0.5%Pd/TiO_2) aqueous solutions of $PdCl_2$ (Sigma Aldrich) and $HAuCl_4$.3-H_2O (Sigma Aldrich) of the desired concentrations were prepared. Polyvinylalcohol (PVA) (1 wt % aqueous solution, Aldrich, MW = 10000, 80% hydrolyzed) and an aqueous solution of $NaBH_4$ (0.1 M) were also prepared. To an aqueous mixture of $PdCl_2$ and $HAuCl_4$ solution of the desired concentration, the required amount of a PVA solution (1 wt %) was added (PVA/(Au+Pd) (w/w) = 1.3). A freshly prepared solution of $NaBH_4$ (0.1 M, $NaBH_4$/(Au+Pd) (mol/mol) = 5) was then added to form a dark-brown sol. After 30 min of sol generation, the colloid was immobilized by adding the support material (TiO_2, Degussa P25; MgO, BDH). For the catalysts prepared with TiO_2 as the support, 1 drop of concentrated H_2SO_4 was added under vigorous stirring. The amount of support material required was calculated so as to have a total final metal loading of 1% wt. The metal ratio for the Au+Pd bimetallic catalyst was 1:1 by weight. After 2 h, the slurry was filtered, and the catalyst was washed thoroughly with 2 L of distilled water (until neutral mother liquors) and then dried at 120 °C overnight under static air.

Conventional Impregnation (C_{Im}). The C_{Im} catalysts were prepared using exactly the same procedure reported by us elsewhere.[19,31,32,41,47] In a typical synthesis of 0.5%Au + 0.5% Pd/TiO_2 catalysts (C_{Im}) the metal precursors were wet impregnated on to the solid support [TiO_2 (Degussa P25, mainly anatase) C (Darco G60, Sigma Aldrich), CeO_2 (<5 μm, Sigma Aldrich), SiO_2 (Grace, Johnson Matthey), MgO (BDH)] using solid $PdCl_2$ (Sigma Aldrich), and $HAuCl_4 \cdot 3H_2O$ (Sigma Aldrich). The requisite amount of solid $PdCl_2$ was added to a predetermined volume of an aqueous solution of $HAuCl_4 \cdot 3H_2O$ and stirred vigorously at 80 °C for a few minutes until the palladium salt had apparently dissolved. After that, the requisite amount of the support was added to this solution under vigorous stirring conditions. The solution was agitated in this way until it formed a paste, which was then dried at 120 °C for 16 h and then calcined in static air, typically at 400 °C for 3 h.

Catalytic Testing. *Direct Synthesis of Hydrogen Peroxide.* Direct synthesis of hydrogen peroxide from hydrogen and oxygen was carried out using standard experimental conditions reported by us in numerous publications.[19,31,32,41,47] Catalyst testing was performed using a stainless steel autoclave (Parr Instruments) with a nominal volume of 100 mL and a maximum working pressure of 14 MPa. The autoclave was equipped with an overhead stirrer (0−2000 rpm) and had a provision for measurement of temperature and pressure. Following the standard reaction conditions we have employed previously, the autoclave was charged with the catalyst (0.01 g) and solvent (5.6 g of MeOH and 2.9 g of H_2O), and purged three times with 5%H_2/CO_2 (3 MPa). It was then filled with 5% H_2/CO_2 and 25% O_2/CO_2 to give a hydrogen/oxygen ratio of 1:2 at a total pressure of 3.7 MPa. Stirring (1200 rpm) was commenced on reaching the desired temperature (2 °C), and experiments were carried out for 30 min. The H_2O_2 yield was determined by titration of aliquots of the final filtered solution with acidified $Ce(SO_4)_2$ (7×10^{-3} mol/L). $Ce(SO_4)_2$ solutions were standardized against $(NH_4)_2Fe(SO_4)_2 \cdot 6H_2O$ using ferroin as indicator.

Solvent-Free Benzyl Alcohol Oxidation. Benzyl alcohol oxidation was carried out in a Radleys carousel reactor using a 50 mL glass stirred reactor. In a typical reaction, the requisite amounts of catalyst and substrate were charged into the reactor at room temperature which was then purged with the required gas (O_2) three times before the reactor was sealed using a Teflon screw threaded cap. The reactor was always connected to the gas-line to ensure the consumed O_2 or He would be topped-up. The pressure was monitored using the pressure gauge fitted in the inlet line to ensure that there was no change in the pressure during the course of the reaction. The reactor with the reaction mixture was loaded into a preheated heating block, which was maintained at the reaction temperature. The reaction started by commencing stirring inside the reactor with a magnetic bar at 1000 rpm. After a specific time, the stirring was stopped and the reactor was immediately cooled in an ice bath. After cooling for 10 min, the reactor was opened slowly and the contents were centrifuged. An aliquot of the clear supernatant reaction mixture (0.5 mL) was then diluted with mesitylene (0.5 mL) for GC analysis. It was also verified that no reaction was occurring in the absence of the Au−Pd catalyst or in the presence of the catalyst support alone. This experimental method is identical to our standard reaction protocols for solvent-free benzyl alcohol oxidation reported elsewhere.[44,45]

Catalyst Characterization. *Scanning Transmission Electron Microscopy (STEM) Analyses.* Samples for examination by scanning transmission electron microscopy were prepared by dry dispersing the catalyst powder onto a holey carbon film supported by a 300 mesh copper TEM grid. STEM high angle annular dark field (HAADF) images and X-ray energy-dispersive spectra of nanoparticles were obtained using an aberration corrected JEOL 2200FS STEM operating at 200 kV. Selected sample powders were also dispersed on an Al-stub and examined in a Hitachi 4300LV SEM equipped with an EDAX energy dispersive X-ray spectrometer.

X-ray Photoelectron Spectroscopy (XPS). XPS measurements were made on a Kratos Axis Ultra DLD spectrometer. Samples were mounted using double-sided adhesive tape, and binding energies were referenced to the C(1s) binding energy of adventitious carbon contamination taken to be 284.7 eV. Monochromatic AlKα radiation was used for all analyses. The intensities of the Au(4f) and Pd(3d) features were used to derive Pd:Au surface molar ratios.

X-ray Diffraction (XRD). Powder X-ray diffraction (XRD) patterns were recorded using a Panalytical X'pert Pro diffractometer using Ni filtered CuKα radiation (operating at 40 kV, 40 mA). Scans were in the range of 10−80° 2θ. The XRD data for all the catalysts are presented in the Supporting Information (Figures S11 and S12).

Conflict of Interest: The authors declare no competing financial interest.

Acknowledgment. The authors acknowledge the EPSRC for funding. M.M. acknowledges the Umm Al-Qura University, Saudi Arabia, for a Ph.D. studentship.

Supporting Information Available: ICP data for the catalysts; effect of reaction temperature on hydrogen peroxide productivity; effect of support identity and heat treatment regime on catalytic performance for C_{Im} and M_{Im} catalysts; additional STEM, and XRD data on the catalysts. This material is available free of charge *via* the Internet at http://pubs.acs.org.

REFERENCES AND NOTES

1. Haruta, M.; Kobayashi, T.; Sano, H.; Yamada, N. Novel Gold Catalysts for the Oxidation of Carbon-Monoxide at a Temperature Far Below 0 °C. *Chem. Lett.* **1987**, 405–408.
2. Hutchings, G. J. Vapor Phase Hydrochlorination of Acetylene: Correlation of Catalytic Activity of Supported Metal Chloride Catalysts. *J. Catal.* **1985**, *96*, 292–295.
3. Choudhary, T. V.; Goodman, D. W. Oxidation Catalysis by Supported Gold Nano-clusters. *Top. Catal.* **2002**, *21*, 25–34.
4. Haruta, M.; Yamada, N.; Kobayashi, T.; Iijima, S. Gold Catalysts Prepared by Co-precipitation for Low-Temperature Oxidation of Hydrogen and of Carbon Monoxide. *J. Catal.* **1989**, *115*, 301–309.
5. Bond, G. C.; Thompson, D. T. Catalysis by Gold. *Catal. Rev., Sci. Eng.* **1999**, *41*, 319–388.
6. Haruta, M.; Daté, M. Advances in the Catalysis of Au Nanoparticles. *App. Catal. A: Gen.* **2001**, *222*, 427–437.
7. Carrettin, S.; Concepción, P.; Corma, A.; López Nieto, J. M.; Puntes, V. F. Nanocrystalline CeO_2 Increases the Activity of Au for CO Oxidation by Two Orders of Magnitude. *Angew. Chem., Intl. Ed.* **2004**, *43*, 2538–2540.
8. Fu, Q.; Saltsburg, H.; Flytzani-Stephanopoulos, M. Active Nonmetallic Au and Pt Species on Ceria-Based Water–Gas Shift Catalysts. *Science* **2003**, *301*, 935–938.
9. Landon, P.; Ferguson, J.; Solsona, B. E.; Garcia, T.; Carley, A. F.; Herzing, A. A.; Kiely, C. J.; Golunski, S. E.; Hutchings, G. J. Selective Oxidation of CO in the Presence of H_2, H_2O and CO_2 *via* Gold for Use in Fuel Cells. *Chem. Commun.* **2005**, 3385–3387.
10. Corma, A.; Garcia, H. Supported Gold Nanoparticles as Catalysts for Organic Reactions. *Chem. Soc. Rev.* **2008**, *37*, 2096–2126.
11. Corma, A.; Serna, P. Chemoselective Hydrogenation of Nitro Compounds with Supported Gold Catalysts. *Science* **2006**, *313*, 332–334.
12. Della Pina, C.; Falletta, E.; Prati, L.; Rossi, M. Selective Oxidation Using Gold. *Chem. Soc. Rev.* **2008**, *37*, 2077–2095.
13. Edwards, J. K.; Hutchings, G. J. Palladium and Gold–Palladium Catalysts for the Direct Synthesis of Hydrogen Peroxide. *Angew. Chem., Int. Ed.* **2008**, *47*, 9192–9198.
14. Corma, A.; Juarez, R.; Boronat, M.; Sanchez, F.; Iglesias, M.; Garcia, H. Gold Catalyzes the Sonogashira Coupling Reaction without the Requirement of Palladium Impurities. *Chem. Commun.* **2011**, *47*, 1446–1448.
15. Enache, D. I.; Edwards, J. K.; Landon, P.; Solsona-Espriu, B.; Carley, A. F.; Herzing, A. A.; Watanabe, M.; Kiely, C. J.; Knight, D. W.; Hutchings, G. J. Solvent-free Oxidation of Primary Alcohols to Aldehydes using Au-Pd/TiO_2 Catalyst. *Science* **2006**, *311*, 362–365.
16. Kobayashi, H.; Yamauchi, M.; Ikeda, R.; Kitagawa, H. Atomic-Level Pd-Au Alloying and Controllable Hydrogen-Absorption Properties in Size-Controlled Nanoparticles Synthesized by Hydrogen Reduction. *Chem. Commun.* **2009**, 4806–4808.
17. Alayoglu, S.; Nilekar, A. U.; Mavrikakis, M.; Eichhorn, B. Ru–Pt Core–Shell Nanoparticles for Preferential Oxidation of Carbon Monoxide in Hydrogen. *Nat. Mater.* **2008**, *7*, 333–338.
18. Ferrando, R.; Jellinek, J.; Johnston, R. L. Nanoalloys: From Theory to Applications of Alloy Clusters and Nanoparticles. *Chem. Rev.* **2008**, *108*, 845–910.
19. Enache, D. I.; Edwards, J. K.; Landon, P.; Solsona-Espriu, B.; Carley, A. F.; Herzing, A. A.; Watanabe, M.; Kiely, C. J.; Knight, D. W.; Hutchings, G. J. Solvent-free Oxidation of Primary Alcohols to Aldehydes Using Au-Pd/TiO_2 Catalysts. *Science* **2006**, *311*, 362–365.
20. Daniel, M. C.; Astruc, D. Gold Nanoparticles: Assembly, Supramolecular Chemistry, Quantum-Size-Related Properties, and Applications Toward Biology, Catalysis, and Nanotechnology. *Chem. Rev.* **2004**, *104*, 293–346.
21. Campelo, J. M.; Luna, D.; Luque, R.; Marinas, J. M.; Romero, A. A. Sustainable Preparation of Supported Metal Nanoparticles and Their Applications in Catalysis. *ChemSusChem* **2009**, *2*, 18–45.
22. Zanella, R.; Giorgio, S.; Henry, C. R.; Louis, C. Alternative Methods for the Preparation of Gold Nanoparticles Supported on TiO_2. *J. Phys. Chem. B* **2002**, *106*, 7634–7642.
23. Okumura, M.; Nakamura, S.; Tsubota, S.; Nakamura, T.; Azuma, M.; Haruta, M. Chemical Vapor Deposition of Gold on Al_2O_3, SiO_2, and TiO_2 for the Oxidation of CO and of H_2. *Catal. Lett.* **1998**, *51*, 53–58.
24. Serpell, C. J.; Cookson, J.; Ozkaya, D.; Beer, P. D. Core@Shell Bimetallic Nanoparticle Synthesis *via* Anion Coordination. *Nat. Chem.* **2011**, *3*, 478–483.
25. Villa, A.; Wang, D.; Su, D. S.; Prati, L. Gold Sols as Catalysts for Glycerol Oxidation: The Role of Stabilizer. *ChemCatChem* **2009**, *1*, 510–514.
26. Comotti, M.; Li, W.-C.; Spliethoff, B.; Schüth, F. Support Effect in High Activity Gold Catalysts for CO Oxidation. *J. Am. Chem. Soc.* **2005**, *128*, 917–924.
27. Li, W. C.; Comotti, M.; Schüth, F. Highly Reproducible Syntheses of Active Au/TiO_2 Catalysts for CO Oxidation by Deposition–Precipitation or Impregnation. *J. Catal.* **2006**, *237*, 190–196.
28. Baatz, C.; Decker, N.; Prüße, U. New Innovative Gold Catalysts Prepared by an Improved Incipient Wetness Method. *J. Catal.* **2008**, *258*, 165–169.
29. Zheng, N.; Stucky, G. D. A General Synthetic Strategy for Oxide-Supported Metal Nanoparticle Catalysts. *J. Am. Chem. Soc.* **2006**, *128*, 14278–14280.
30. Yan, W.; Brown, S.; Pan, Z.; Mahurin, S. M.; Overbury, S. H.; Dai, S. Ultrastable Gold Nanocatalyst Supported by Nanosized Non-oxide Substrate. *Angew. Chem., Int. Ed.* **2006**, *45*, 3614–3618.
31. Edwards, J. K.; Solsona, B.; N, E. N.; Carley, A. F.; Herzing, A. A.; Kiely, C. J.; Hutchings, G. J. Switching-Off Hydrogen Peroxide Hydrogenation in the Direct Synthesis Process. *Science* **2009**, *323*, 1037–1041.
32. Edwards, J. K.; Carley, A. F.; Herzing, A. A.; Kiely, C. J.; Hutchings, G. J. Direct Synthesis of Hydrogen Peroxide From H_2 and O_2 Using Supported Au–Pd Catalysts. *Faraday Discuss.* **2008**, *138*, 225–239.
33. Haruta, M. Gold as a Novel Catalyst in the 21st Century: Preparation, Working Mechanism and Applications. *Gold Bull.* **2004**, *37*, 27–36.
34. Lopez-Sanchez, J. A.; Dimitratos, N.; Hammond, C.; Brett, G. L.; Kesavan, L.; White, S.; Miedziak, P.; Tiruvalam, R.; Jenkins, R. L.; Carley, A. F.; Knight, D.; Kiely, C. J.; Hutchings, G. J. Facile Removal of Stabilizer-Ligands from Supported Gold Nanoparticles. *Nat. Chem.* **2011**, *3*, 551–556.
35. Carabineiro, S. A. C.; Thompson, D. T. Catalytic Applications for Gold Nanotechnology. *Nanocatalysis* **2007**, 377–489.
36. Kung, H. H.; Kung, M. C.; Costello, C. K. Supported Au Catalysts for Low Temperature CO Oxidation. *J. Catal.* **2003**, *216*, 425–432.
37. Oh, H. S.; Yang, J. H.; Costello, C. K.; Wang, Y. M.; Bare, S. R.; Kung, H. H.; Kung, M. C. Selective Catalytic Oxidation of CO: Effect of Chloride on Supported Au Catalysts. *J. Catal.* **2002**, *210*, 375–386.
38. Kung, M. C.; Davis, R. J.; Kung, H. H. Understanding Au-Catalyzed Low-Temperature CO Oxidation. *J. Phys. Chem. C* **2007**, *111*, 11767–11775.
39. Bowker, M.; Nuhu, A.; Soares, J. High Activity-Supported Gold Catalysts by Incipient Wetness Impregnation. *Catal. Today* **2007**, *122*, 245–247.
40. Ivanova, S.; Petit, C.; Pitchon, V. A New Preparation Method for the Formation of Gold Nanoparticles on an Oxide Support. *Appl. Catal. A: Gen.* **2004**, *267*, 191–201.
41. Pritchard, J. C.; He, Q.; Ntainjua, E. N.; Piccinini, M.; Edwards, J. K.; Herzing, A. A.; Carley, A. F.; Moulijn, J. A.; Kiely, C. J.; Hutchings, G. J. The Effect of Catalyst Preparation Method on the Performance of Supported Au–Pd Catalysts for the Direct Synthesis of Hydrogen Peroxide. *Green Chem.* **2010**, *12*, 915–921.
42. Pritchard, J.; Kesavan, L.; Piccinini, M.; He, Q.; Tiruvalam, R.; Dimitratos, N.; Lopez-Sanchez, J. A.; Carley, A. F.; Edwards, J. K.; Kiely, C. J.; Hutchings, G. J. Direct Synthesis of Hydrogen Peroxide and Benzyl Alcohol Oxidation Using Au–Pd Catalysts Prepared by Sol Immobilization. *Langmuir* **2010**, *26*, 16568–16577.

43. Hashimoto, N.; Takahashi, Y.; Hara, T.; Shimazu, S.; Mitsudome, T.; Mizugaki, T.; Jitsukawa, K.; Kaneda, K. Fine Tuning of Pd^0 Nanoparticle Formation on Hydroxyapatite and Its Application for Regioselective Quinoline Hydrogenation. *Chem. Lett.* **2010**, *39*, 832–834.
44. Meenakshisundaram, S.; Nowicka, E.; Miedziak, P. J.; Brett, G. L.; Jenkins, R. L.; Dimitratos, N.; Taylor, S. H.; Knight, D. W.; Bethell, D.; Hutchings, G. J. Oxidation of Alcohols Using Supported Gold and Gold−Palladium Nanoparticles. *Faraday Discuss.* **2010**, *145*, 341–356.
45. Sankar, M.; Nowicka, E.; Tiruvalam, R.; He, Q.; Taylor, S. H.; Kiely, C. J.; Bethell, D.; Knight, D. W.; Hutchings, G. J. Controlling the Duality of the Mechanism in Liquid-Phase Oxidation of Benzyl Alcohol Catalysed by Supported Au−Pd Nanoparticles. *Chem.—Eur. J.* **2011**, *17*, 6524–6532.
46. Tiruvalam, R. C.; Pritchard, J. C.; Dimitratos, N.; Lopez-Sanchez, J. A.; Edwards, J. K.; Carley, A. F.; Hutchings, G. J.; Kiely, C. J. Aberration Corrected Analytical Electron Microscopy Studies of Sol-Immobilized Au + Pd, Au{Pd} and Pd{Au} Catalysts Used for Benzyl Alcohol Oxidation and Hydrogen Peroxide Production. *Faraday Discuss.* **2011**, *152*, 63–86.
47. Edwards, J. K.; Solsona, B. E.; Landon, P.; Carley, A. F.; Herzing, A.; Kiely, C. J.; Hutchings, G. J. Direct Synthesis of Hydrogen Peroxide from H_2 and O_2 Using TiO_2-Supported Au−Pd Catalysts. *J. Catal.* **2005**, *236*, 69–79.
48. Herzing, A. A.; Watanabe, M.; Edwards, J. K.; Conte, M.; Tang, Z.-R.; Hutchings, G. J.; Kiely, C. J. Energy Dispersive X-ray Spectroscopy of Bimetallic Nanoparticles in an Aberration Corrected Scanning Transmission Electron Microscope. *Faraday Discuss.* **2008**, *138*, 337–351.
49. Chang, F.-W.; Yu, H.-Y.; Selva Roselin, L.; Yang, H.-C. Production of Hydrogen *via* Partial Oxidation of Methanol Over Au/TiO_2 Catalysts. *Appl. Catal. A: Gen.* **2005**, *290*, 138–147.
50. Konova, P.; Naydenov, A.; Venkov, C.; Mehandjiev, D.; Andreeva, D.; Tabakova, T. Activity and Deactivation of Au/TiO_2 Catalyst in CO Oxidation. *J. Mol. Catal. A: Chem.* **2004**, *213*, 235–240.
51. Arrii, S.; Morfin, F.; Renouprez, A. J.; Rousset, J. L. Oxidation of CO on Gold Supported Catalysts Prepared by Laser Vaporization: Direct Evidence of Support Contribution. *J. Am. Chem. Soc.* **2004**, *126*, 1199–1205.
52. Radnik, J.; Mohr, C.; Claus, P. On the Origin of Binding Energy Shifts of Core Levels of Supported Gold Nanoparticles and Dependence of Pretreatment and Material Synthesis. *Phys. Chem. Chem. Phys.* **2003**, *5*, 172–177.
53. Liu, R.; Yu, Y.; Yoshida, K.; Li, G.; Jiang, H.; Zhang, M.; Zhao, F.; Fujita, S.-i.; Arai, M. Physically and Chemically Mixed TiO_2-Supported Pd and Au Catalysts: Unexpected Synergistic Effects on Selective Hydrogenation of Citral in Supercritical CO_2. *J. Catal.* **2010**, *269*, 191–200.
54. Venezia, A. M.; Liotta, F. L.; Pantaleo, G.; Beck, A.; Horváth, A.; Geszti, O.; Kocsonya, A.; Guczi, L. Effect of Ti(IV) Loading on CO Oxidation Activity of Gold on TiO_2 Doped Amorphous Silica. *Appl. Catal. A: Gen.* **2006**, *310*, 114–121.
55. Egelhoff, W. F., Jr.; Tibbetts, G. G. Growth of Copper, Nickel, and Palladium Films on Graphite and Amorphous Carbon. *Phys. Rev. B* **1979**, *19*, 5028–5035.
56. Wang, H.-F.; Ariga, H.; Dowler, R.; Sterrer, M.; Freund, H.-J. Surface Science Approach to Catalyst Preparation—Pd Deposition onto Thin Fe_3O_4(111) Films from $PdCl_2$ Precursor. *J. Catal.* **2012**, *286*, 1–5.
57. Shen, Y.; Wang, S.; Huang, K. Effects of Chloride Precursors on the Palladium Valency and Surface Structures of $PdMg_2/SiO_2$ Catalysts for Carbon Monoxide Hydrogenation. *Appl. Catal.* **1990**, *57*, 55–70.